A Comparison of Segmental Dynamics in Polymers by Solid-State ^{13}C NMR Spectroscopy

K. J. McGrath,* K. L. Ngai, and C. M. Roland

Code 6120, Naval Research Laboratory, Washington, D.C. 20375-5342

Received October 12, 1994; Revised Manuscript Received February 2, 1995®

ABSTRACT: The temperature dependences of the line widths observed in solid-state ^{13}C NMR spectra for several polymers are shown to correlate with the time and temperature dependences of the segmental dispersions in their dielectric relaxation spectra. The NMR line width variations arise from molecular motions which modulate the $^{1}H-^{13}C$ dipolar interaction and the chemical shift anisotropy (CSA), thus interfering with the proton decoupling of the dipolar interaction and the magic angle spinning modulation of the CSA. These same motions govern the local segmental dynamics, and hence there is a direct connection between the results from macroscopic probes of polymer relaxation such as dielectric spectroscopy and microscopy measurements like NMR. The polymers studied herein exhibit a range of segmental relaxation properties, ranging from narrow relaxation functions with weak temperature dependences to very broad relaxation spectra whose mean relaxation times change markedly with temperature. In the ^{13}C NMR experiments these behaviors correspond to line broadening over very wide or narrow temperature ranges, respectively. Our analysis demonstrates the manner in which solid-state NMR spectroscopy can provide information on the segmental dynamics of polymers, interpretable in the framework of relaxation models.

Introduction

Solid-state ^{13}C nuclear magnetic resonance (NMR) spectroscopy employing magic angle spinning (MAS) and high-power radio-frequency proton decoupling provides a direct microscopic probe of local chain dynamics in neat polymers[1-4] and blends.[5,6] In a recent paper[7] we applied this technique to measure the segmental dynamics of two polymers, polyisobutylene (PIB) and poly(vinylethylene) (PVE), which have contrasting properties as revealed by various macroscopic probe experiments, including mechanical,[8-12] dielectric,[13] and photon correlation spectroscopies.[14] For PIB, the local relaxation spectrum, as well as the retardation spectrum, when isolated from the Rouse modes' contribution has a very narrow dispersion, and the measured relaxation time, τ, has a weak temperature dependence. In contrast, local segmental relaxation of PVE is associated with a considerably broader spectral dispersion and stronger sensitivity to temperature. A measure of this temperature sensitivity of τ is seen in an Arrhenius plot (see Figure 9) with the temperature normalized by the glass transition temperature, T_g. The latter is taken to be the temperature at which τ reaches an arbitrary time, e.g., 100 s. The validity of this approach (referred to as cooperativity or fragility plots) for comparing temperature dependencies of different polymers has been amply demonstrated.[8,15,16] The strong correlation of the temperature sensitivity of τ with the breadth of the glass transition dispersion has been established[9,15,16] for a wide variety of organic polymers through the use of these cooperativity plots. The origin of this correlation has been suggested[17] to be intermolecular cooperativity associated with the local segmental relaxation which determines both the breadth of the dispersion and the temperature dependency of τ.

Our previous solid-state ^{13}C NMR investigations of neat PIB and PVE showed that the molecular motions underlying their respective segmental relaxations have very different temperature dependencies,[7] paralleling the result from macroscopic probes. In view of these results, we have extended the NMR measurements to a wide variety of polymers, including poly(vinyl chloride) (PVC), which has the strongest temperature dependency and the broadest segmental relaxation dispersion of any organic polymer.[9,15-20] With PVC and PIB representing the two extremes of maroscopic relaxation behavior, we also investigated poly(vinyl acetate) (PVAc) and polyisoprene (PIP), which are intermediate in the breadth of their relaxation spectrum and temperature dependency, and poly(vinylethylene) (PVE), which has a broad spectral dispersion, but still narrower than that of PVC. The consequences of these varying segmental dynamics on the solid-state ^{13}C NMR response near and above the polymers' glass transition temperatures are described.

Experimental Section

All NMR spectra were obtained on a Bruker MSL 300 spectrometer with a static magnetic field of 7.04 T (300.1 MHz ^{1}H and 75.5 MHz ^{13}C Larmor frequencies). A double-tuned multinuclear magic angle spinning (MAS) probehead equipped for 7 mm o.d. sample rotors was used to acquire all spectra. A waiting time of 15 min at each temperature was allowed in order for sample and probe to reach thermal equilibrium. Probehead input impedance was readjusted after temperature equilibration immediately prior to data acquisition. The Hartmann–Hahn cross polarization (CP) technique[21] was employed at temperatures where a sufficient static heteronuclear dipolar interaction was available for efficient cross polarization, using proton decoupling during acquisition of the carbon free induction decay. At higher temperatures, a single carbon-13 $\pi/2$ pulse (5 μs) was used with proton decoupling.[22] The ^{13}C NMR spectra were acquired in increments of 2 °C over the entire temperature range where the peaks were observed to undergo broadening due to interference by segmental relaxation. All spectra were obtained using magic angle spinning[23,24] maintained at 3.0 kHz ± 5 Hz. Observe (^{13}C) and decoupling (^{1}H) radio-frequency fields for cross polarization and one-pulse experiments were maintained at 50 kHz, and a cross polarization contact time of 1 ms was used in all CP experiments, with a relaxation delay of 2 s. No apodization of the free induction decay was employed in any of the experiments.

® Abstract published in *Advance ACS Abstracts,* March 15, 1995.

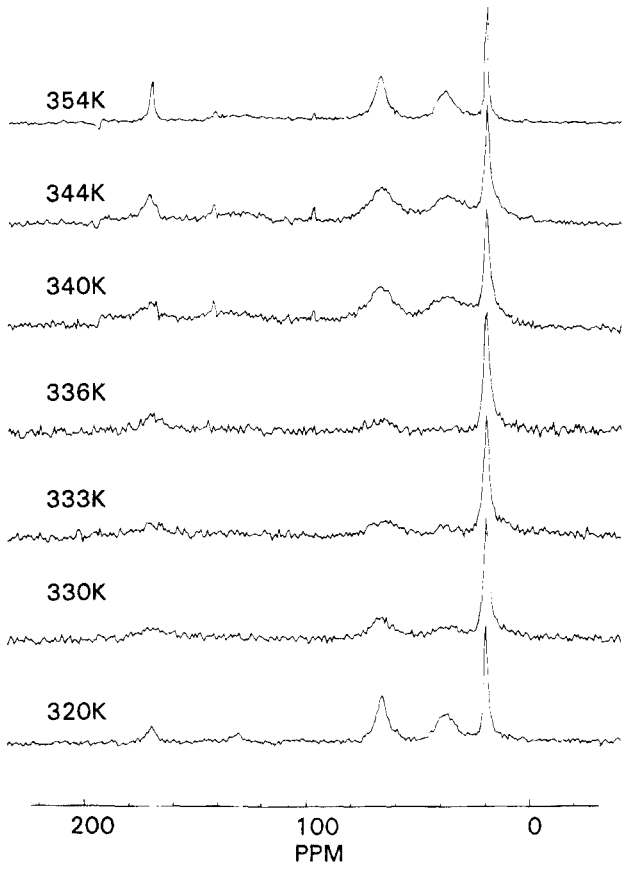

Figure 1. Carbon-13 NMR spectra of neat PVAc obtained over the temperature range 320–354 K. The backbone methine and methylene carbon resonances are at δ = 67 and 39 ppm, respectively, and the carbonyl carbon appearas at δ = 170 ppm. These peaks broaden over the temperature range 324–352 K due to the presence of 3–50 kHz segmental reorientation. The pendant methyl carbon at 21 ppm does not undergo broadening in this temperature range due to rapid C3 reorientation.

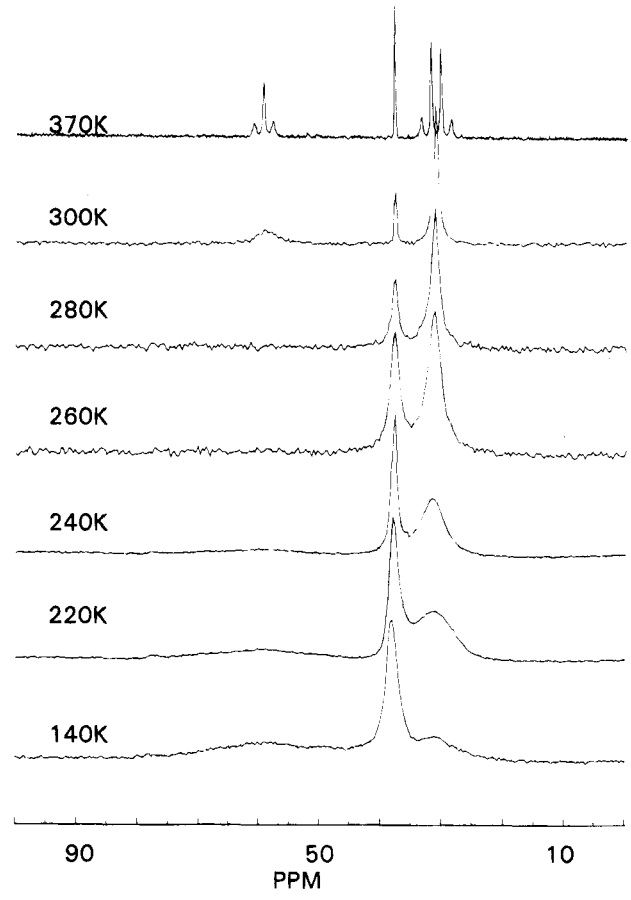

Figure 2. Carbon-13 NMR spectra of neat PIB obtained over the temperature range 140–370 K. The peaks at δ = 31, 38, and 59 ppm correspond to the methyl, quaternary, and methylene carbons, respectively. The broadening of the quaternary carbon in the 260–300 K temperature range is primarily attributed to 3–50 kHz segmental relaxation. The spectrum at 370 K was obtained without proton decoupling for peak assignment purposes.

Results

Figures 1–3 show representative carbon-13 NMR spectra of PVAc, PIB, and PVC obtained over the temperature range for which their respective backbone carbon resonances undergo broadening as a result of segmental relaxation (*vide infra*). Magic angle spinning (3 kHz) is used in the acquisition of these spectra so that the variation in chemical shift (chemical shift anisotropy (CSA)) associated wtih molecular orientation in the applied static magnetic field B_0 is modulated to its isotropic average. In addition, a 50 kHz radio-frequency (RF) proton decoupling field is applied during acquisition of the carbon free induction decay to average the heteronuclear dipole–dipole interaction among carbon and hydrogen nuclei. Without MAS and proton RF irradiation, resolution of the chemically distinct carbon resonances would not be possible due to the absence of isotropic motional averaging on the time scale of the chemical shift anisotropy and heteronuclear dipolar interactions in these samples (at temperatures in the vicinity of T_g).

When the polymer motions transpire over the critical 3–50 kHz time scale, the localized fluctuating magnetic fields generated by the reorienting segments interfere with the MAS modulation of chemical shift anisotropy and/or the proton RF irradiation modulation of the carbon–proton dipolar interaction. The diminished averaging of these interactions results in line broadening of the individual peaks in the ^{13}C NMR spectrum (corresponding to the chemically distinct nuclei of the polymer). The fraction of segments (and thus nuclei) reorienting on the 3–50 kHz time scale will obviously depend upon sample temperature. When reorientational time scales are either short (higher temperature) or long (lower temperature) compared with the MAS or RF decoupling period, no inteference with the modulation of CSA or heteronuclear dipolar interaction occurs, and the ^{13}C NMR peak resonances are narrow (at least in the absence of other line broadening contributions). The peaks broaden only over the temperature range for which the segmental relaxation frequencies are within the critical 3–50 kHz range for a significant fraction of the sample. Thus, we are able to decipher the temperature range over which segmental motions in the polymers are occurring at or near the time scale of the MAS spin rate (3 kHz) and/or the proton RF decoupling field (50 kHz).

The PVAc ^{13}C NMR spectrum shown in Figure 1 at 320 K evidences a relatively narrow resonance at 67 ppm (corresponding to the backbone methine carbon) with $\delta\nu_{1/2} \approx$ 380 Hz. This peak does not narrow significantly as temperature is lowered below 320 K. However, as shown, higher temperature (above 320 K) results in the onset of peak broadening, due to the presence of segmental relaxation on the 3–50 kHz time scale. Maximum line width occurs at approximately 336 K (37 K above the calorimetric glass transition), because the spectral density of segmental relaxation on the 3–50

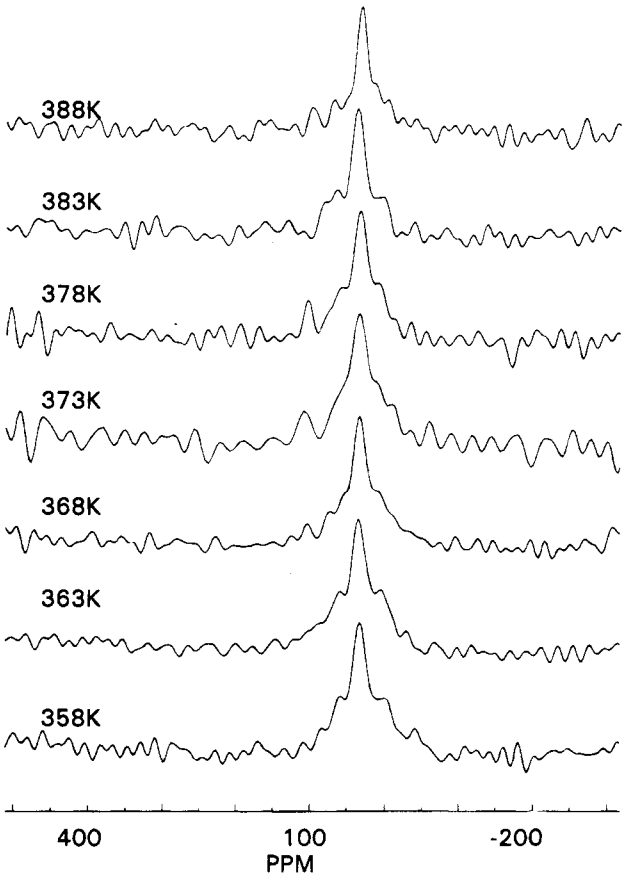

Figure 3. Carbon-13 NMR spectra of neat PVC obtained over the temperature range 358–388 K. Although the individual methylene (δ = 45 ppm) and methine (δ = 57 ppm) carbon resonances cannot be resolved, line broadening due to 3–50 kHz segmental relaxation occurs between the relatively narrow temperature range 368–383 K.

kHz time scale is highest at this temperature. As temperature is further increased, the methine carbon resonance begins to narrow as the time scale of segmental relaxation becomes short relative to the MAS and proton decoupling periods. At 352 K, the line width has decreased to its width at 324 K because segmental motions are now rapid relative to the critical 3–50 kHz time scale. The temperature range in neat PVAc for which a relatively large fraction of the sample is undergoing segmental relaxation on the 3–50 kHz time scale is 324–352 K (ΔT = 28° K); the line width is therefore dominated by these motions in this temperature interval. The lower and upper temperature limits of peak broadening will hereafter be referred to as T_L and T_H-respectively.

The methylene backbone carbon of PVAc (e.g., $-CH_2-$ at 39 ppm) exhibits a dependence of its segmental relaxation on temperature, similar to that of the methine carbon, as does the pendant carbonyl carbon at 170 ppm. The pendant methyl group at 21 ppm does not undergo significant line broadening in the 324–352 K range because of the rapid rate (relative to 3–50 kHz) of C3 rotation over this temperature interval. The large-scale 3–50 kHz segmental motions discussed above all occur at temperatures significantly above the calorimetric T_g of 299 K, where the spectral density is sufficiently high to produce extreme line broadening. No segmental relaxation mechanism for line broadening to such a degree exists below T_g in any of the homopolymers studied herein, except at temperatures where methyl groups rotate at the critical 3–50 kHz frequency. These temperatures are far below the calorimetric T_g in all samples herein and therefore are neglected in our analysis.

Figure 2 shows the ^{13}C NMR results for neat PIB over the temperature range 140–370 K. The pendant methyl carbon at 31 ppm is observed to progressively broaden as temperature is lowered below 370 K because the frequency of C3 rotation approaches the 3–50 kHz range at lower temperatures. However, even at 140 K the peak width has not maximized due to the still relatively rapid rate of C3 rotational reorientation at this temperature (*vide infra*). The quaternary backbone carbon resonance of PIB at 38 ppm exhibits only moderate line broadening between 260 and 300 K. This is not surprising given the weak heteronuclear dipolar interaction at a carbon lacking directly bonded hydrogen. Nonetheless, the broadening of this resonance between 260 and 300 K is indicative of reorientation on the 3–50 kHz time scale at this site and the adjacent (protonated) methylene backbone carbon. The magnitude of chemical shift anisotropy of this saturated carbon must also be small, and no strong interactions exist for extreme line broadening, regardless of the time scale of reorientation. The adjacent methylene backbone carbon of PIB at 59 ppm contains two directly bonded hydrogens, and therefore a large potential heteronuclear dipolar interaction and line-broadening mechanism. As shown in Figure 2, this carbon resonance begins broadening above 300 K and is never observed to narrow significantly as temperature is lowered toward 140 K. We have previously shown that this line broadening is not attributable to an inhomogeneous mechanism,[7] such as would occur if there were a wide dispersion of chemical shifts. However, this line broadening cannot be solely attributed to the interference of 3–50 kHz segmental relaxation with MAS or proton decoupling since the methylene resonance *remains* broad below the calorimetric glass transition temperature of 200 K, where the spectral density of these backbone motions must be very low. As previously discussed, one type of motion with potentially high spectral density in the critical 3–50 kHz range *below* T_g is C3 methyl rotation. However, a previous study of PIB has shown that the rate of rotation of the methyl groups is *rapid* relative to the 3–50 kHz range, *even at 140 K*.[7] No other motions exist which could contribute the necessary spectral density in the 3–50 kHz regime for significant line broadening below T_g. We expect the extreme line broadening observed in the methylene carbon resonance between 260 and 300 K to be attributable primarily to 3–50 kHz reorientational motion as seen for the adjacent quaternary carbon over this temperature interval.

Figure 3 shows the ^{13}C NMR spectra of neat PVC obtained over the temperature range 358–388 K. The quality factor of our NMR probe at these elevated temperatures was significantly diminished and precluded the acquisition of extremely high signal-to-noise spectra in a time interval consistent with precise MAS rates and (magnet bore) heat control. Nonetheless, we obtained line width data at 2 K temperature increments and trends in line width variation are clearly visible. The separate methylene (45 ppm in solution) and methine (57 ppm in solution) carbon resonances of PVC are not resolvable at any of the temperatures shown. The breadth of these resonances is in part a consequence of the relatively wide distribution of isotropic chemical shifts, as evidenced by the broad nature of both methylene and methine carbons of PVC *solution-state* NMR spectra (not shown). The peak width in the absence of motional line broadening (e.g., 2200 Hz at 358 K,

Table 1. Segmental Relaxation Data from ^{13}C NMR Resonance Line-Broadening Experiments and Dielectric Relaxation Spectra

polymer	T_g[a] (K)	^{13}C line-broadening range[b] (K) ($T_H - T_L$)	β[c]
PVAc	305	324–352 (ΔT = 28 K)	0.43
PIB	200	~260–300 ($\Delta T \approx$ 40 K)	0.55
PVC	354	368–383 (ΔT = 15 K)	0.25
PIP	200	232–262 (ΔT = 30 K)	0.50
PVE	270	286–317 (ΔT = 31 K)	0.41

[a] Glass transition temperature determined by differential scanning calorimetry. [b] Temperature range over which ^{13}C NMR resonance line broadening occurs in *backbone* carbon resonances. See text for further details. [c] Stretch exponent β (eq 1) determined from dielectric spectroscopy.

determined on the composite methylene/methine resonance far exceeds that of the individual peak separations of 900 Hz (determined from solution-state experiments). Most signficantly, only a minor extent of line broadening attributable to segmental relaxation on the 3–50 kHz time scale is present and is apparent only within the narrow temperature range of 368 K (T_L) to 383 K (T_H), where the peak width has increased to approximately 3000 Hz (at 375 K). Nonetheless, both the methine and methylene carbons of PVC contain *directly bonded hydrogen* which must provide a strong heteronuclear dipolar interaction, and therefore a significant segmental relaxational line-broadening mechanism. The absence of extreme ^{13}C NMR line broadening in PVC suggests that there is a relatively low spectral density of 3–50 kHz motion at any given temperature (between 368 and 383 K). The spectral density is widely dispersed whereby only a fraction at any temperature contributes to the NMR line broadening.

As described above, PIB, PVAc, and PVC vary widely in their macroscopic segmental relaxation behavior, and hence the divergent microscopic ^{13}C NMR results are not unexpected. The ^{13}C NMR results for all of the polymers, including data for PIP and PVE (spectra in ref 5), are summarized in Table 1.

Discussion

Arrhenius plots for the PVAc, PIB, PVC, PIP, and PVE segmental relaxation times are shown respectively in Figures 4–8. The *macroscopic* segmental relaxation times τ were determined from the maxima in the respective dielectric loss spectra at each temperature for PVE,[13] PIP,[13,25] PVAc,[26] and PVC;[19,20] τ for PIB was determined from photon correlation spectroscopy.[14] Also shown in Figures 4–8 are the isothermal dielectric loss, ϵ'', spectra at the low- and high-temperature limits (T_L and T_H) of peak broadening as determined from solid-state ^{13}C NMR experiments. The scales for the ϵ'' spectra are not marked but correspond exactly to the inverse of the main ordinate, $\log(\tau)$. The two dotted lines indicate the angular frequencies of 3 and 50 kHz, that is, the range of the NMR frequency window. The dielectric spectra shown in Figures 4–8 are actually fits of experimental data to the Fourier transform of the time derivative of the Kohlrausch–William–Watts (KWW) function,[27,28]

$$\theta(t) \sim \exp\left[-\left(\frac{t}{\tau}\right)^{\beta}\right] \qquad (0 < \beta < 1) \qquad (1)$$

The original dielectric data were taken at a number of

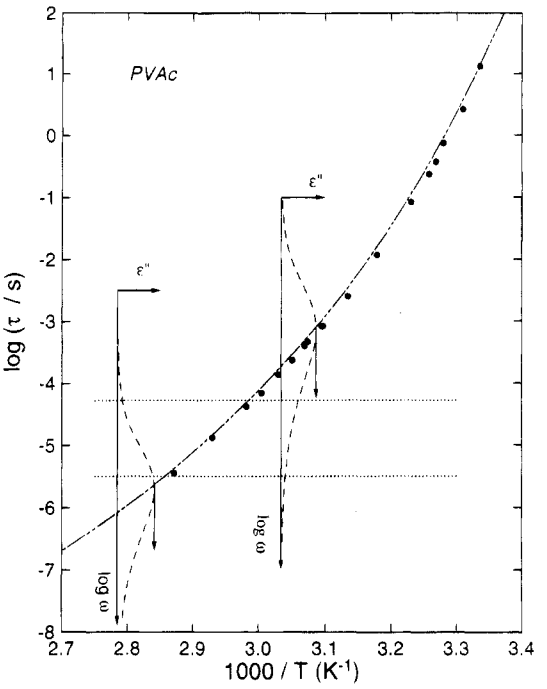

Figure 4. Most probable relaxation time τ of the segmental motion correlation function of PVAc approximated by the KWW function plotted against reciprocal temperature. The points represent experimental data while the curve through the points is the Vogel–Fulcher fit to the temperature dependence of τ. The two vertical arrows pointing downward indicate the locations of $1000/T_L$ and $1000/T_H$. The insets are isothermal loss spectra, $\epsilon''(\omega)$, plotted against $\log \omega$ at T_L and T_H. The scale of the $\log \omega$ axis of the figure in the inset is exactly the same as that of the ordinate, $\log(\tau/s)$ of the main figure. For this reason the τ-curve of the main figure intersects the maxima of the ϵ'' curves (dashed) at values of the abscissa equal to $1000/T_L$ and $1000/T_H$. The two horizontal dotted lines indicate the two critical time scales for broadening in the ^{13}C NMR experiment (3 and 50 kHz).

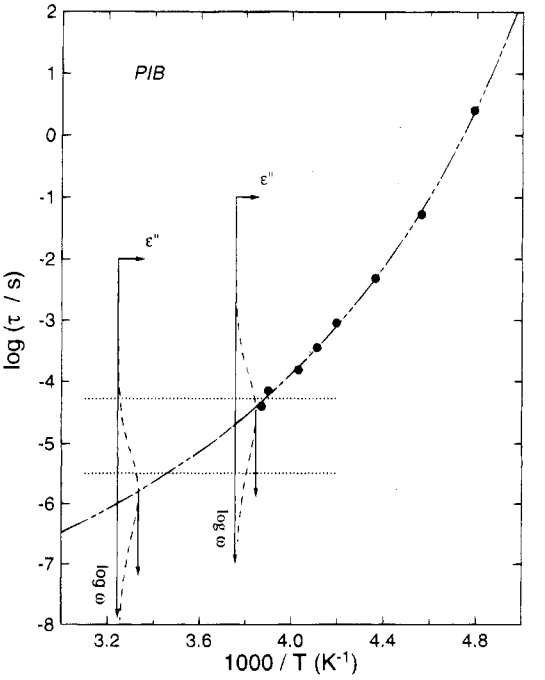

Figure 5. Same as for Figure 4, except the polymer is now PIB and the loss data are obtained from dielectric spectroscopy (ref 24).

temperatures not necessarily coincident with T_L and T_H. The locations of these two temperatures on the $1000/T$ axis are indicated by the vertical arrows emanating from

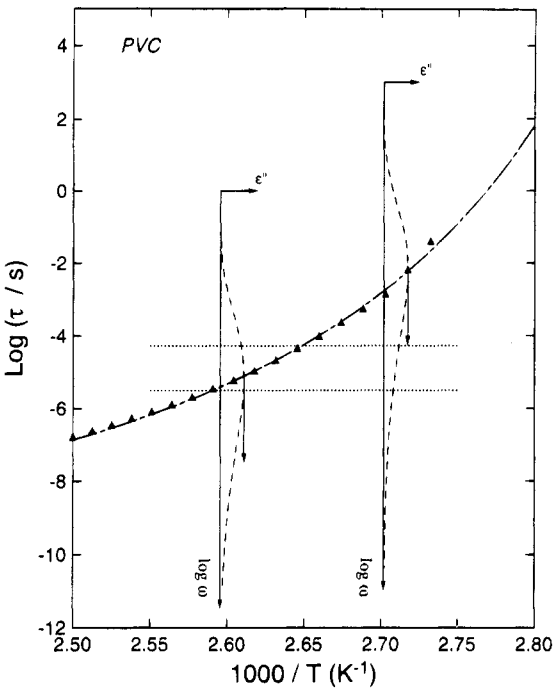

Figure 6. Same as for Figure 4, except the polymer is now PVC and the loss data are obtained from dielectric spectroscopy (ref 25).

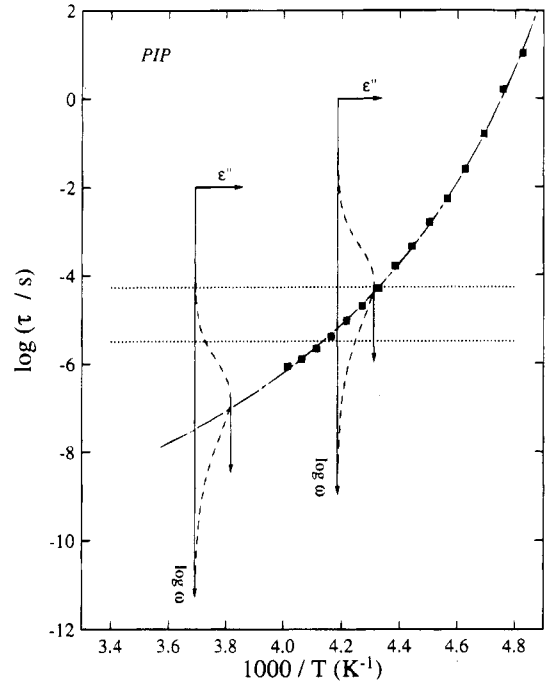

Figure 7. Same as for Figure 4, except the polymer is now PIP and the loss data are obtained from dielectric spectroscopy (refs 12 and 14).

the ϵ'' peak. The solid curve in Figures 4–8 are the fits of the temperature dependence of the most probable relaxation time τ to the Vogel–Fulcher equation.[28] The points of intersection of this solid curve with the tips of the two vertical arrows in each of these figures locate the τ's for T_L and T_H, respectively. With both τ and the stretch exponent β known, the macroscopic dielectric loss at T_L and T_H can be calculated by Fourier transform of the derivative of the KWW function given by eq 1. In this manner we obtain the dielectric loss spectral intensity at T_L and T_H relative to the two critical frequencies for line broadening of the ^{13}C NMR experiments. The stretch exponent β is related to the width

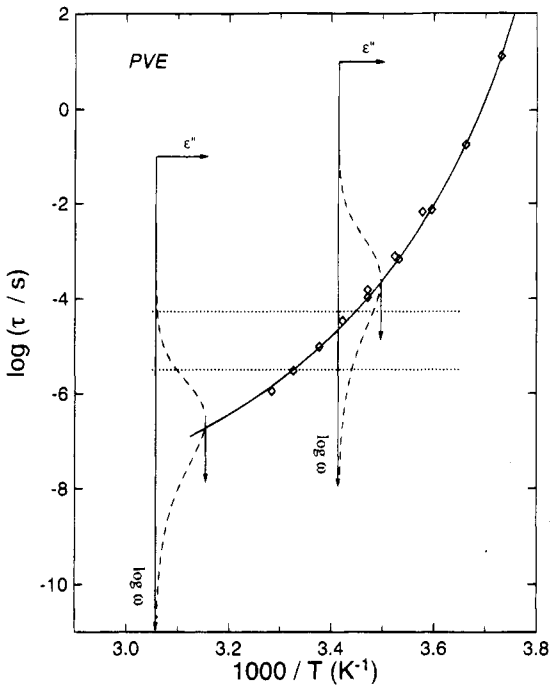

Figure 8. Same as for Figure 4, except the polymer is now PVE and the loss data are obtained from dielectric spectroscopy (refs 18 and 19).

W (in decades) of the frequency-domain relaxation spectrum by $\beta \approx 1.14/W$.[2] The portion of the macroscopic relaxation spectral intensity (dashed curve) within these frequency limits indicates the fraction of the distribution of the segmental relaxation process which lies inside the 3–50 kHz frequency window.

Examination of Figures 4–8 reveals a close correspondence between the measured time scales of macroscopic (dielectric loss, photon correlation spectroscopy) and microscopic (NMR) segmental relaxation for each of the samples. The majority of the macroscopic spectral dispersion for each sample (≥70%, within the region $\epsilon'' \geq 0.1\epsilon''_{max}$) passes through the critical 3–50 kHz NMR frequency window as temperature is varied between T_L and T_H. That is, for most samples, no less than approximately 70% of the area defined by the macroscopic spectral dispersions (determined at T_L and T_H) falls within the critical 3–50 kHz NMR line-broadening frequency range over the temperature interval T_L to T_H. Thus, in general, the microscopic reorientational relaxation which governs the ^{13}C NMR line broadening occurs over the temperature interval inferred from the macroscopic relaxation measurements.

As indicated above, the breadths of the macroscopic relaxation functions vary considerably among the polymers. Those for PIB, PIP, and PVAc are relatively narrow ($\delta\nu_{1/2} \approx 2.1$–$2.3$ decades of frequency), $\theta(t)$ is somewhat broader for PVE (2.8 decades)[30] and much broader in PVC (4.9 decades). Since the present ^{13}C NMR technique is sensitive to motions only in the frequency range 3–50 kHz, broader dispersions will contribute proportionally less spectral density within this range at any given temperature. In the case of PIB, PVAc, PIP, and PVE, the spectral distribution that lies within the critical 3–50 kHz NMR line-broadening window is in the range of ~50–65% between T_L and T_H. In contrast, the extremely wide dispersion of PVC allows at most only 25% to fall within the critical NMR line-broadening window. The lack of substantial line broadening in the ^{13}C NMR resonances of PVC is a direct consequence of its broad relaxation spectrum.

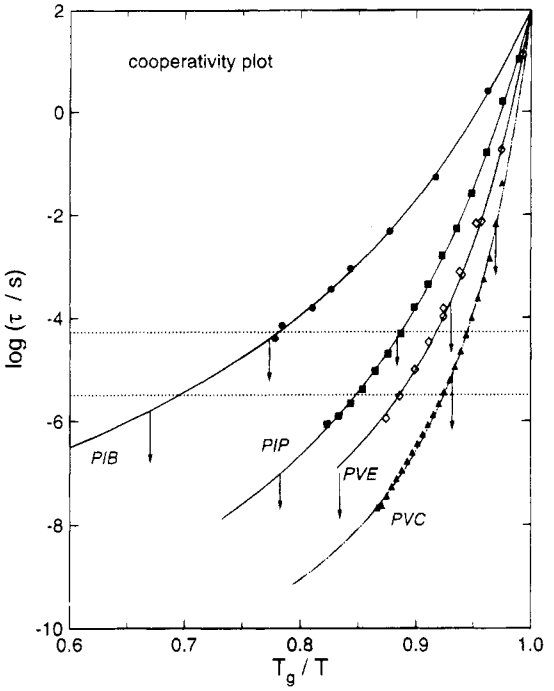

Figure 9. Cooperativity plot of τ against T_g/T for four polymers. The vertical arrows pointing downward indicate the locations of T_g/T_L and T_g/T_H. The horizontal dotted lines indicate the two critical time scales for broadening in the ^{13}C NMR experiments.

Finally, we compare the relaxation times of the various polymers in a "cooperativity plot"[8,9,15,16] (Figure 9), where T_g is defined as the temperature at which τ assumes the value of 10^2 s. As before, the horizontal dotted lines represent the upper (3 kHz) and lower (50 kHz) bounds of the ^{13}C NMR line-broadening window. The temperature locations of the two intersections of the τ (solid) curve with the dotted lines (which define the temperature where the segmental dynamics are occurring on the time scale defined by the MAS and RF decoupling frequencies) correlate reasonably well with the NMR T_L and T_H for each polymer. Although it is gratifying to find such a correlation, we do not expect these locations to be exactly coincident. In Figure 9 the vertical arrows indicate the normalized temperature limits for NMR line broadening (T_g/T_L and T_g/T_H). In particular, Figure 9 shows that the more cooperative polymers, having a steeper decrease of log τ with normalized reciprocal temperature T_g/T, are characterized by intersections with the dotted lines at higher values of T_g/T. In addition, a decrease in the KWW β parameter (eq 1) also accompanies greater τ-dependence, as indicated by the temperature excursions between the critical NMR line-broadening time scales. Thus, the temperature range associated with NMR line broadening can be directly related to the shape of a polymer's cooperativity curve.

Summary

Given the complexity of polymer dynamics, insights gained from a single experimental technique are very limited, or can even be misleading. Progress in understanding the relaxation behavior of polymers requires multiple approaches which complement and corroborate one another. The analysis presented herein demonstrates that the temperature dependence of the line width observed in solid-state ^{13}C NMR (with MAS and proton decoupling) is the same as the temperature dependence of the segmental relaxation determined from bulk measurements such as dielectric spectroscopy. Aside from trivial exceptions to this correlation (due, for example, to pendant group motions), any differences in the respective temperature dependencies measured by the two techniques are a consequence of the different time windows accessed by the experiments.

As shown by many prior studies, relaxation dynamics having broad dispersions in dielectric or mechanical spectra are associated with relaxation times which change markedly with temperature. The latter behavior results in NMR line broadening occurring over only a relatively narrow range, corresponding to the range of temperatures for which significant spectral density falls within the NMR frequency window. Hence, broad spectral dispersions as seen by macroscopic techniques appear as narrow NMR resonances over a greater range of temperatures than do narrow spectral dispersions.

Acknowledgment. This work was supported by the Office of Naval Research, K.L.N. under Contract N0001494WX23010, and K.J.M. and C.M.R. under Contract N0001495WX40001.

References and Notes

(1) Garroway, A. N.; Moniz, W. B.; Resing, H. A. *ACS Symp. Ser.* **1979**, *No. 103*.
(2) Garroway, A. N.; Ritchey, W. M.; Moniz, W. B. *Macromolecules* **1982**, *15*, 1051.
(3) Henrichs, M. P.; Nicely, V. A. *Macromolecules* **1991**, *24*, 2506.
(4) Lyerla, J. R.; Yannoni, C. S. *IBM J. Res. Dev.* **1983**, *27*, 302.
(5) Miller, J. B.; McGrath, K. J.; Roland, C. M.; Trask, C. A.; Garroway, A. N. *Macromolecules* **1990**, *23*, 4535.
(6) Takegoshi, K.; Hikichi, K. *J. Chem. Phys.* **1991**, *94*, 3200.
(7) McGrath, K. J.; Ngai, K. L.; Roland, C. M. *Macromolecules* **1992**, *25*, 4911.
(8) Roland, C. M.; Ngai, K. L. *Macromolecules* **1992**, *25*, 5765.
(9) Plazek, D. J.; Ngai, K. L. *Macromolecules* **1991**, *24*, 1222.
(10) Plazek, D. J.; Zheng, X. D.; Ngai, K. L. *Macromolecules* **1992**, *25*, 4920.
(11) Ngai, K. L.; Plazek, D. J.; Bero, C. A. *Macromolecules* **1993**, *26*, 1065.
(12) Plazek, D. J.; Ngai, K. L.; Roland, C. M., to be published.
(13) Colmenero, J.; Alegría, A.; Ngai, K. L.; Roland, C. M. *Macromolecules* **1994**, *27*, 407.
(14) Rizos, A. K.; Jian, T.; Fytas, G.; Ngai, K. L. *Macromolecules*, in press.
(15) Böhmer, R.; Ngai, K. L.; Angell, C. A.; Plazek, D. J. *J. Chem. Phys.* **1993**, *99*, 4201.
(16) Ngai, K. L.; Roland, C. M. *Macromolecules* **1993**, *26*, 6824.
(17) For a recent review, see: Nagi, K. L. In *Disorder Effects on Relaxation Processes, Glasses, Polymers, Proteins*; Richert, R., Blumen, A., Eds.; Springer-Verlag: Berlin, 1994; pp 89–150.
(18) Ngai, K. L.; Yee, A. F. *J. Polym. Sci., Part B: Polym. Phys.* **1991**, *29*, 1493.
(19) Colmenero, J. *Physica A* **1993**, *201*, 38.
(20) Colmenero, J.; Arbe, A.; Alegria, A. *Phys. Rev. Lett.* **1993**, *71*, 2603.
(21) Hartmann, S. R.; Hahn, E. L. *Phys. Rev.* **1962**, *128*, 2042.
(22) Sarles, L. R.; Cotts, R. M. *Phys. Rev.* **1958**, *111*, 853.
(23) Andrew, E. R. *Arch. Sci.* **1959**, *12*, 103.
(24) Lowe, I. J. *Phys. Rev. Lett.* **1959**, *2*, 285.
(25) Algría, A.; Colmenero, J.; Ngai, K. L.; Roland, C. M. *Macromolecules* **1994**, *27*, 4486.
(26) Nozaki, R.; Mashimo, S. *J. Chem. Phys.* **1986**, *84*, 3575.
(27) Kohlrausch, R. *Pogg. Ann. Phys.* **1854**, *91*, 179.
(28) Williams, G.; Watts, D. C. *Trans. Faraday Soc.* **1970**, *66*, 80.
(29) Ferry, J. D. *Viscoelastic Properties of Polymers*; Wiley: New York, 1980.
(30) Roland, C. M. *Macromolecules* **1994**, *27*, 4242.

MA946042N